Journal of Applied Mechanics and Technical Physics, Vol. 42, No. 1, pp. 125–130, 2001

FORMATION OF NONMETALLIC INCLUSIONS OF VARIABLE COMPOSITION DURING UNIDIRECTIONAL SOLIDIFICATION OF LIQUID STEEL

A. N. Cherepanov, V. N. Popov, S. I. Plaksin,[1] and A. A. Kazakov[2]

UDC 669.18.046.518-412

A two-dimensional unsteady mathematical model is presented for numerical study of the formation of nitrogen-containing compounds of variable composition during unidirectional solidification of liquid steel. The model allows calculation of the distributions of temperature and concentrations of soluble admixtures, the shape of solidification boundaries, the coordinate of the beginning of the chemical reaction, and the composition and mass of inclusions formed in the uncrystallized zone of the ingot and in the two-phase region.

Introduction. The quality of metal production may be improved and the cost may be reduced by using nitrogen to form a dispersed-composite structure of cast metal. The results of [1–3] show that even small quantities of nitrogen and nitride-forming elements significantly improve the mechanical and physicochemical properties of steel and alloys. However, the positive effect of nitrides on the quality of the metal is manifested only for concentrations of nitrogen and nitride-forming elements typical of a particular alloy. If these concentrations are significantly different from the optimal values, the metal properties may become worse. Therefore, the problem of finding the optimal concentrations of nitride-forming metals and nitrogen and the study of the structure and dispersion of endogenous inclusions, being related to the processes of formation of the dendritic structure of the solidifying alloy, become extremely important.

In the present paper we consider an unsteady two-dimensional mathematical model for studying the formation of nitrogen-containing compounds of variable composition during continuous extension of a steel ingot in a tubular container.

1. Physical Formulation of the Problem. We consider the process of crystallization of a multispecies alloy located in an axisymmetric crucible-container (Fig. 1). The crucible with the alloy is extended downward with a constant velocity v from the zone of the heater toward the cooler and then is cooled in a gaseous medium. The outer surface of the crucible is separated from the inner surface of the cooler (which is a copper shell with cooling water circulating over an annular channel) by a gas gap of width δ_{c}. There is also a gap of width δ_{h} between the crucible and the heater. Disk screens are placed in the region separating the lower face of the heater from the upper face of the cooler.

2. Governing Equations and Boundary Conditions. We use a coordinate system (r, z), where the z axis coincides with the axis of symmetry of the ingot, and the origin is the intersection of the z axis with the plane of the upper face of the cooler. The z axis is directed downward and coincides with the direction of ingot extension. Ignoring the diffusion of components dissolved in the liquid and solid phases and the shrinkage phenomena during phase transition, we write the heat- and mass-transfer equations in the approximation of the theory of the quasiequilibrium two-phase zone [3, 4]:

Institute of Theoretical and Applied Mechanics, Siberian Division, Russian Academy of Sciences, Novosibirsk 630090. [1]Novosibirsk State Pedagogical University, Novosibirsk 630126. [2]St. Petersburg State Technical University, St. Petersburg 195251. Translated from Prikladnaya Mekhanika i Tekhnicheskaya Fizika, Vol. 42, No. 1, pp. 140–146, January–February, 2001. Original article submitted February 3, 2000.

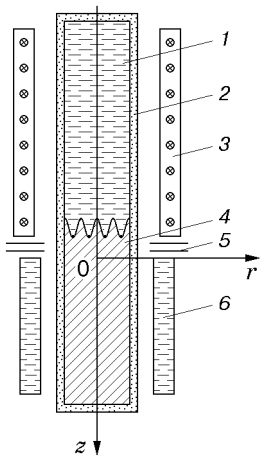

Fig. 1. Layout of the facility for studying unidirectional crystallization of steel: 1) liquid metal; 2) crucible; 3) heater; 4) ingot; 5) screens; 6) cooler.

$$c^i\rho^i\,\frac{dT}{dt}=\frac{1}{r}\,\frac{\partial}{\partial r}\Big(\lambda^i r\,\frac{\partial T}{\partial r}\Big)+\frac{\partial}{\partial z}\Big(\lambda^i\,\frac{\partial T}{\partial z}\Big)+æ_0\rho^1\,\frac{df_{\rm liq}}{dt};\tag{1}$$

$$\frac{dC_j}{dt}=-(1-k_j)C_j\,\frac{d(\ln\,f_{\rm liq})}{dt}-\frac{1}{\rho^1 f_{\rm liq}}\,\frac{\overline{dI_\nu}}{dt},\qquad \nu=1,2,\ldots,m;\tag{2}$$

$$T=T_A-\sum_{j=1}^{N-1}\beta_j C_j,\qquad j=1,2,3,\ldots,N-1;\tag{3}$$

$$\begin{gathered}f_{\rm liq}\equiv 1\quad\text{for}\quad T>T^0_{\rm liq},\qquad f_{\rm liq}\equiv 0\quad\text{for}\quad T<T_E,\\ i=1\quad\text{for}\quad r\in[0,r_1],\qquad i=2,\quad f_{\rm liq}\equiv 0\quad\text{for}\quad r\in[r_1,r_2].\end{gathered}\tag{4}$$

Here T is the temperature, T_A is the melting point of the pure solvent component, $T^0_{\rm liq}$ and T_E are the temperatures of the beginning and end of solidification of the melt, $æ_0$ is the crystallization heat, c^i, ρ^i, and λ^i are the heat capacity, density, and thermal conductivity, respectively, r_1 and r_2 are the ingot and crucible radii, t is the time, $f_{\rm liq}$ is the fraction of the liquid phase, C_j is the concentration, k_j is the coefficient of distribution of the jth dissolved component, N is the number of components in the alloy, m is the number of components participating in chemical reactions, and β_j is the absolute value of the angular coefficient of the liquidus line of the alloy of the jth component and iron; the superscript i indicates physical quantities that refer to the ingot ($i=1$) and the crucible ($i=2$); $d/dt=\partial/\partial t+v\partial/\partial z$. The first term in the right part of Eq. (2) denotes capturing of the jth dissolved component by the growing solid phase; the second term is the velocity of transition (binding) of the νth reagent into a nonmetallic inclusion during its growth in the two-phase region. The quantity $\overline{dI_\nu}/dt$ characterizes the velocity of transition of the νth component to a chemical compound of variable composition, averaged over the cross section of the dendritic cell.

To obtain the dependence of $\overline{dI_\nu}/dt$ on the physical parameters of the solidifying alloy, we introduce the following notation: $n_{\rm comp}$ is the number of molecules of compounds in a unit volume, $A_\Sigma=\sum x_\nu A_\nu$ is the molecular weight of the compound, and x_ν and A_ν are, respectively, the molar concentration and atomic weight of the νth element in the compound. Let $\mu_\nu=x_\nu A_\nu$ be the total atomic weight of the νth element in a molecule of the compound. A mass of the νth element $dI_\nu=d(n_{\rm comp}\mu_\nu)$ is bound into a nonmetallic inclusion in a unit volume during the time dt. Passing to the mass fraction of inclusions formed in the dendritic cell $M=n_{\rm comp}A_\Sigma/\rho^1$, we obtain

$$\frac{dI_\nu}{dt}=\frac{\rho^1 d(MY_\nu)}{dt},\tag{5}$$

where ρ^1 is the steel density, which is assumed to be independent of the aggregate state and temperature, and $Y_\nu = x_\nu A_\nu / A_\Sigma$ are the fractions of atomic weights of reagents in the compound. We now define the quantity $\overline{dI_\nu}/dt$ averaged over the cross section of the dendritic cell by the relation

$$\overline{\frac{dI_\nu}{dt}} = \frac{2}{a_0^2}\int\limits_R^{a_0} \frac{dI_\nu}{dt}\, r\, dr = \frac{2}{a_0^2}\left(\frac{d}{dt}\int\limits_R^{a_0} I_\nu r\, dr + \bar{I}_{\nu R} R \frac{dR}{dt}\right),$$

where $\bar{I}_{\nu R}$ is the mean value of I_ν over the dendrite boundary and a_0 and R are the cell and dendrite radii, respectively. For certainty, we assume that dendrites have a columnar structure. Taking into account that $f_{\text{liq}} = (a_0^2 - R^2)/a_0^2$, we represent the latter relation as

$$\overline{\frac{dI_\nu}{dt}} = \frac{d(f_{\text{liq}}\langle I_\nu\rangle)}{dt} - \bar{I}_{\nu R}\frac{df_{\text{liq}}}{dt}, \tag{6}$$

where $\langle I_\nu\rangle = \dfrac{2}{a_0^2 - R^2}\displaystyle\int\limits_R^{a_0} I_\nu r\, dr$ is the mean value of I_ν over the cross section of the liquid phase. Then ,we assume that $\bar{I}_{\nu R} = \langle I_\nu\rangle$. From (6), taking into account Eq. (5), after appropriate transformations, we find

$$\overline{\frac{dI_\nu}{dt}} = f_{\text{liq}}\frac{d\langle I_\nu\rangle}{dt} = \rho^1 f_{\text{liq}}\frac{d\langle MY_\nu\rangle}{dt}.$$

Substituting this expression into Eq. (2) and omitting the angular brackets for averaged quantities, we obtain the mass-transfer equation for the reacting components:

$$\frac{dC_j}{dt} = -(1-k_j)C_j\frac{d(\ln f_{\text{liq}})}{dt} - \frac{d(MY_\nu)}{dt}. \tag{7}$$

The distributions of concentrations of the components in the region where there are no chemical reactions and the distributions of concentrations of the components that do not participate in the reactions are found from Eq. (7) for $M \equiv 0$.

For certainty, we consider a five-species ($N = 5$) iron-based alloy (Fe+C+Ti+Cr+N) whose solidification is accompanied by formation of carbonitride compounds of variable composition of the type $\text{TiC}_x\text{N}_{1-x}$. Then we obtain the following relations for Y_ν:

$$Y_1 = A_1/A_\Sigma, \qquad Y_2 = xA_2/A_\Sigma, \qquad Y_3 = (1-x)A_3/A_\Sigma. \tag{8}$$

Here $A_\Sigma = A_1 + xA_2 + (1-x)A_3$; the subscripts $\nu = 1$, 2, and 3 refer to Ti, C, and N, respectively.

The conditions of equilibrium of the reaction of inclusion formation and equilibrium of its composition in the approximation of an ideal solution lead to the equations [2]

$$x = 1 + C_3K_{13}/(C_2K_{12}), \qquad C_1C_2 = (1-x)/K_{13}, \tag{9}$$

where K_{12} and K_{13} are the equilibrium constants of simple compounds TiC and TiN, respectively, the expressions for which were prescribed in accordance with [2, 5, 6].

Following [7], we determine the liquidus temperature of the alloy considered:

$$T_{\text{liq}} = 1812 - 78C_{\text{C}} - 10C_{\text{Ti}} - 90C_{\text{N}} - 1.5C_{\text{Cr}}$$

(C_{C}, C_{Ti}, C_{N}, and C_{Cr} are the concentrations of the corresponding components).

System (1), (7), (3), (4), taking into account relations (8) and (9), is solved for the following boundary conditions:

$$T_1 = T_2 = T_{\text{h}}, \qquad t = 0, \qquad z \in [-z_+^0, -z_-^0],$$

$$T\Big|_{r=r_1-0} = T\Big|_{r=r_1+0}, \qquad \lambda^1\frac{\partial T}{\partial r}\Big|_{r=r_1-0} = \lambda^2\frac{\partial T}{\partial r}\Big|_{r=r_1+0},$$

$$-\lambda^2\frac{\partial T}{\partial r}\Big|_{r=r_2} = \alpha_1(T)(T\Big|_{r=r_2} - T_{\text{h}}), \qquad z \in [z_+(t), -z_{\text{h}}], \tag{10}$$

$$-\lambda^2 \frac{\partial T}{\partial r}\Big|_{r=r_2} = \varepsilon_n \sigma_0 (T^4\Big|_{r=r_2} - T_{\rm s}^4), \qquad z \in [-z_{\rm h}, 0],$$

$$-\lambda^2 \frac{\partial T}{\partial r}\Big|_{r=r_2} = \alpha_2(T)(T\Big|_{r=r_2} - T_{\rm c}), \quad z \in [0, z_-(t)], \qquad \frac{\partial T}{\partial r}\Big|_{r=0} = 0, \quad z \in [z_+(t), z_-(t)],$$

$$\frac{\partial T}{\partial z}\Big|_{z=z_+(t)} = 0, \quad r \in [0, r_2], \qquad -\lambda^2 \frac{\partial T}{\partial z}\Big|_{z=z_-(t)} = \varepsilon_{nj} \sigma_0 (T^4\Big|_{z=z_-} - T_j^4), \quad r \in [0, r_2].$$

Here $\alpha_j = \lambda_{\rm g}/\delta_j + \varepsilon_{nj}\sigma_0(T^2\Big|_{r=r_2} + T_j^2)(T\Big|_{r=r_2} + T_j)$ are the heat-transfer coefficients, which characterize the complex heat transfer by radiation and heat conduction of the gas between the outer surface of the crucible and inner surfaces of the heater ($j \equiv$ h) and the cooler ($j \equiv$ c), $\lambda_{\rm g}$ is the heat conductivity of the gas, $\varepsilon_{nj} = (\varepsilon_t^{-1} + \varepsilon_j^{-1} - 1)^{-1}$, ε_t, $\varepsilon_{\rm h}$, and $\varepsilon_{\rm c}$ are the emissivities of the crucible, heater, and cooler, respectively, $\sigma_0 = 5.67 \cdot 10^{-8}$ W/(m$^2\cdot$K^4) is the Stefan–Boltzmann constant, $T_{\rm h}$, $T_{\rm c}$, and $T_{\rm s}$ are the prescribed temperatures of the inner surfaces of the heater, cooler, and screening surfaces in the gap separating the lower face of the heater from the upper face of the cooler (Fig. 1), $-z_{\rm h}$ is the coordinate of the lower face of the heater, and $z_+(t)$ and $z_-(t)$ are the laws of motion of the upper and lower faces of the crucible prescribed in the form of linear functions of the time t: $z_+(t) = -z_+^0 + vt$ and $z_-(t) = -z_-^0 + vt$. It is assumed that the crucible with the melt is completely located in the zone of the heater at the initial time, and the surface of the lower face of the crucible is located in the plane of the lower face of the heater ($z = -z_{\rm h}$).

The diameter of the dendritic cell $d_1 = 2a_0$ in the steady regime is determined by the empirical relation [8]

$$d_1 = b_{10} G^{-\gamma} v_{\rm cr}^{-s},$$

where G is the temperature gradient averaged along the two-phase region, b_{10}, γ, and s are empirical constants, and $v_{\rm cr}$ is the local crystallization velocity (for unidirectional solidification, we have $v_{\rm cr} = v$).

The initial system of equations with the boundary conditions (10) was solved numerically with the help of an implicit difference scheme approximating the initial system with an error of order $O(\tau, h^2)$. The calculations were performed on a 25×90 uniform grid in the r and z directions, respectively. The variable time step τ was chosen from the conditions of stability of numerical calculation and convergence of iterations and varied from 10^{-2} to 10^{-3} sec. To solve the systems of algebraic equations obtained at each time step, we used the methods of block sequential upper relaxation (with an optimal iteration parameter) and simple iterations. The calculations were terminated when the relative error reached $\varepsilon = 0.002$.

3. Analysis of Results. Some results of numerical simulation are plotted in Figs. 2–5 for different ingot-extension velocities and initial concentrations of nitrogen in the steady regime of crystallization. The calculations were performed for the following initial data:

— alloy parameters $C_{10} = C_{\rm Ti}^0 = 0.5\%$, $C_{20} = C_{\rm C}^0 = 0.06\%$, $C_{30} = C_{\rm N}^0 = 0.002$ and 0.005%, $C_{40} = C_{\rm Cr}^0 = 14.4\%$, $T_A = 1802$ K, $T_E = 1760$ K, $\beta_1 = 10$ K/%, $\beta_2 = 78$ K/%, $\beta_3 = 90$ K/%, $\beta_4 = 1.5$ K/%, $k_1 = 0.7$, $k_2 = 0.4$, $k_3 = 0.38$, $k_4 = 0.91$, $\lambda^1 = 23$ W/(m $\cdot$ K), $c^1 = 694$ J/(kg $\cdot$ K), $\rho^1 = 7.2 \cdot 10^3$ kg/m^3, $æ_0 = 3.37 \cdot 10^5$ J/kg, $b_{10} = 1.52 \cdot 10^{-2}$ m $\cdot$ (K/sec)$^{0.26}$, $s = 0.26$, and $\gamma = 0.46$;

— crucible parameters $\lambda^2 = 8.721$ W/(m $\cdot$ K), $c^2 = 838$ J/(kg $\cdot$ K), $\rho^2 = 1.5 \cdot 10^3$ kg/m^3, $\varepsilon_t = 0.15$, $\delta_t = 1.5 \cdot 10^{-3}$ m, $l_t = 90 \cdot 10^{-3}$ m, and $r_2 = 5 \cdot 10^{-3}$ m;

— heater and cooler parameters $T_{\rm h} = 1923$ K and $\varepsilon_{\rm h} = 0.9$, $T_{\rm c} = 333$ K and $\varepsilon_{\rm c} = 0.8$, $\delta_{\rm c} = 1.5 \cdot 10^{-3}$ m and $\delta_{\rm h} = 2 \cdot 10^{-3}$ m, and $\lambda_{\rm g} = 0.02$ W/(m $\cdot$ K).

The change in the temperature $T_{\rm s}$ in the gap between the upper face of the cooler and the lower face of the heater is set by the linear function $T_{\rm s} = T_{\rm h} + (T_{\rm h} - T_{\rm c})z/z_{\rm h}$, where $z_{\rm h} = 0.02$ m and $z \in [-z_{\rm h}, 0]$. When the crucible is moved down to the cooler, the melt is cooled and solidifies in the bottom-to-top direction. The width and morphology of the two-phase region change due to the tip effect until the process of solidification reaches the steady regime. This regime occurs when the length of the solidified metal reaches approximately two diameters of the crucible and remains as long as the temperature of the melt in the upper part of the crucible is constant and equal to the initial value. The morphology of the two-phase region in the regime of

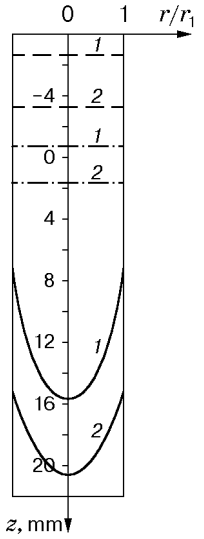

Fig. 2

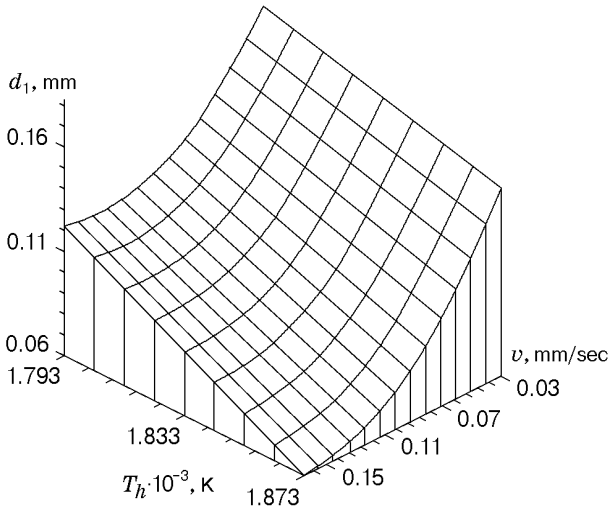

Fig. 3

Fig. 2. Structure of the two-phase region of the ingot for extension velocities $v = 10^{-4}$, $1.167 \cdot 10^{-4}$, and $8 \cdot 10^{-4}$ m/sec (dashed, dot-and-dashed, and solid curves, respectively); the initial and final boundaries of the two-phase region are marked by 1 and 2, respectively.

Fig. 3. Distance d_1 between the major axes of the dendrites versus the ingot-extension velocity and the heater temperature.

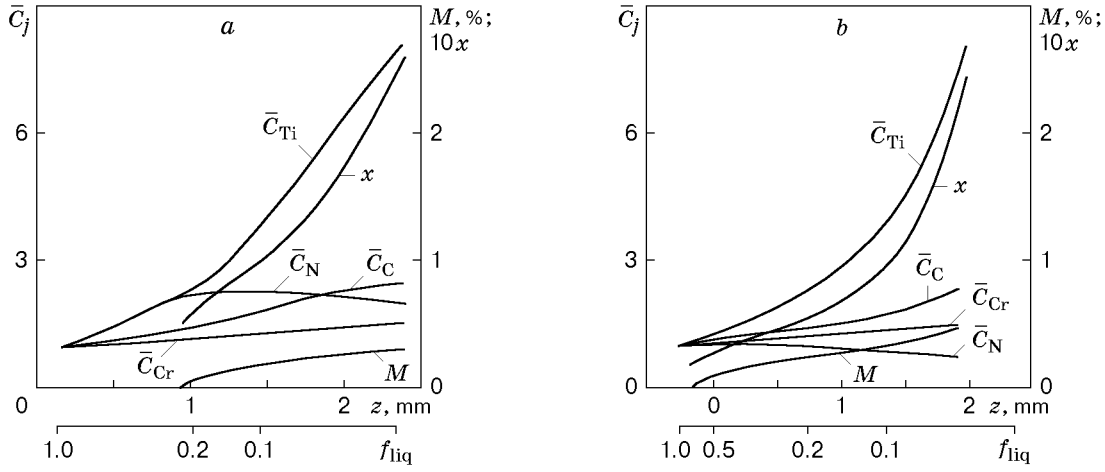

Fig. 4. Lengthwise distributions of the relative concentrations $\bar{C}_j$, composition x, and mass M of $\mathrm{TiC}_x\mathrm{N}_{1-x}$ compounds for $C^0_{\rm N} = 0.002$ (a) and 0.005% (b).

solidification depends significantly on the Peclet number $\mathrm{Pe} = c^1\rho^1 v r_1/\lambda^1$. For $\mathrm{Pe} \ll 1$, the boundaries of the two-phase region are plane (Fig. 2), and the value of G remains unchanged along the radius r. In accordance with this, the primary structure uniform across the ingot is formed.

For $\mathrm{Pe} > 1$, a liquid–solid crater is formed; the quantities G and $v_{\rm cr}$, and hence, the cooling velocity $v_T = Gv_{\rm cr}$ are variable over the radius r. As a result, the ingot cross section becomes structurally inhomogeneous.

Figure 3 shows the dependence of the dendrite-cell size d_1 on the ingot-extension velocity v and the heater temperature $T_{\rm h}$ (or the gradient in the melt). An increase in the dispersion of the structural components is observed with increasing the above-mentioned parameters.

The beginning of the chemical reaction depends significantly on the initial concentration of dissolved nitrogen $C^0_{\rm N}$ (Fig. 4). Thus, for $C^0_{\rm N} = 0.002\%$ and the initial value $C^0_{\rm Ti} = 0.5\%$ ($v_{\rm cr} = 0.167$ mm/sec), the

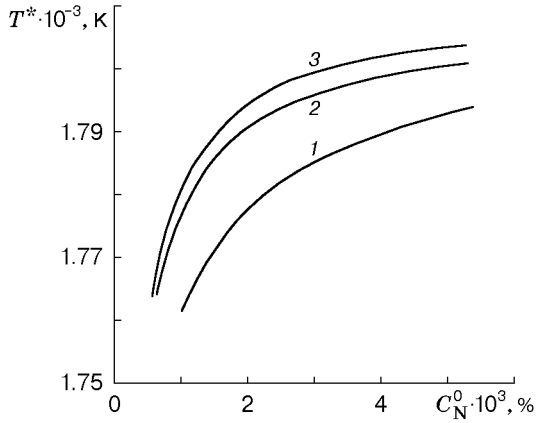

Fig. 5. Temperature of the beginning of the chemical reaction of TiC_xN_{1-x} formation versus the initial concentrations of nitrogen and titanium: $C^0_{Ti} = 0.1$ (1), 0.3 (2), and 0.5% (2).

formation of TiC_xN_{1-x} compounds starts at the point $f^*_{liq} = 0.25$ ($T^* = 1795$ K), and for $C^0_N = 0.005\%$, it begins at the point $f^*_{liq} = 0.885$ ($T^* = 1802$ K). An increase in the nitrogen concentration from 0.002 to 0.005% leads to an increase in the amount of matter TiC_xN_{1-x} (the value of M) from 0.032 to 0.053%.

The composition of the chemical compounds formed changes. We have $x = 0.0467$–0.0156 in the beginning of their formation and $x = 0.266$–0.257 at the end of solidification for $C_N = 0.002$–0.005%. For $C_N > 0.0055\%$, the inclusions arise in the uncrystallized region of the ingot, i.e., ahead of the front of the two-phase region.

Figure 5 shows the temperature of the beginning of the chemical reaction of TiC_xN_{1-x} formation versus the initial concentrations of nitrogen and titanium. An increase in the concentration of nitrogen and titanium elements dissolved in the initial melt leads to an increase in the temperature of the beginning of formation of the chemical compound, i.e., to the shift of the point of TiC_xN_{1-x} formation toward the front of the two-phase region, and hence, to an increase in the inclusion size with an unchanged local cooling velocity of the melt.

Thus, the mathematical model proposed allows one to study the laws of formation of the ingot structure and the formation dynamics, composition, and dispersion of carbonitride compounds of variable composition, which are formed at various stages of cooling and crystallization of a multispecies melt.

REFERENCES

1. Ts. V. Rashev, *Production of Alloyed Steel* [in Russian], Metallurgiya, Moscow (1981).
2. V. A. Grigoryan, L. N. Belyanchikov, and A. Ya. Stomakhin, *Theoretical Fundamentals of Electric Steel-Melting Processes* [in Russian], Metallurgiya, Moscow (1987).
3. V. T. Borisov, "Theory of formation of nonmetallic inclusions in the two-phase region of a crystallizing ingot," in: *Processes of Deoxidation and Formation of Nonmetallic Inclusions in Steel* (collected scientific papers) [in Russian], No. 76, Nauka, Moscow (1977), pp. 72–81.
4. A. N. Cherepanov, "Macroscopic theory of nonequilibrium crystallization of alloys," *Izv. Vyssh. Uchebn. Zaved., Chern. Metallurg.*, No. 4, 50–54 (1988).
5. V. A. Petrovskii, A. E. Volkov, and V. T. Borisov, "Formation of nonmetallic inclusions of variable composition in solidifying steel," *Izv. Vyssh. Uchebn. Zaved., Chern. Metallurg.*, No. 4, 49–52 (1981).
6. A. A. Kazakov, A. Kh. Urazgil'deev, and A. A. Gusev, "Algorithmic model of formation of nonmetallic inclusions in liquid and solidifying steel," *Izv. Akad. Nauk SSSR, Met.*, No. 3, 60–65 (1989).
7. V. A. Denisov and A. V. Denisov, "Method for calculation of steel solidification temperatures," *Litein. Proizv.*, No. 5, 11–13 (1982).
8. H. Jacobi and K. Schwerdfeger, "Dendrite morphology of steady state unidirectionally solidified steel," *Metall. Trans.*, **7A**, 811–820 (1976).